Main Lobe Shaping in Wide-Band Arrays

Simone Curletto and Andrea Trucco

Department of Biophysical and Electronic Engineering (DIBE), University of Genoa
Via all'Opera Pia 11A, I - 16145 Genova (Italy).
Phone: +39 010 353 2035 Fax: +39 010 353 2134 E-mail: curletto@dibe.unige.it

***Abstract* – This paper describes a method to obtain a wide-band beam pattern whose main lobe has a desired shape and, at the same time, an acceptable side lobes level. The aim of our work is to reproduce a main lobe profile as close as possible to a desired one by means of a synthesis of the array weighting window. To achieve this goal, an optimization process based on the simulated annealing is developed. Although the quality of the resulting beam pattern is slightly poorer than the one obtained in narrow-band conditions, the proposed method allows to well attain the desired shape of the main lobe, also in case of flattop shaped beam.**

I. INTRODUCTION

This paper deals with the linear beamforming [1,2], a technique aimed at processing the signals sampled by an array of sensors. Of all the applications that the beamforming method is able to offer here we consider the one referring to the active acoustical imaging systems [2,3].

When the spatial aperture of the array is larger than the equivalent spatial length of the pulse used for the insonification, the beam pattern (BP) profile also depends on the shape of the pulse envelope [3-5]. This case is usually referred to as the "wide-band condition", as it requires pulses of short time duration (i.e., wide-band signals). Images obtained by using wide-band pulses are generally of a higher quality (the range resolution gets better) and potentially contain more information than those obtained when narrow-band is considered [2,3]. Besides, wide-band signals allow to avoid a typical problem related to the narrow-band systems and consisting of the presence of grating lobes in the BP [3-5] that arise when the array elements are equispaced and the inter-element spacing is larger than $\lambda/2$ (λ being the wavelength related to the carrier frequency). However, in wide-band conditions the definition of BP is not just one [4-6]. Of all the possible definitions, here the BP is defined as the maximum over the time of every beam signal absolute value.

This paper describes a method to obtain a BP that performs two different constraints: a desired main lobe profile and an acceptable side lobes level. In particular, our aim is to reproduce a BP in wide-band conditions with a main lobe similar to the so called "shaped beam", i.e. a BP in which the main lobe shows a flat top instead of a rapid descent [7]. Although in narrow-band conditions several methods have been proposed to synthesize a weighting window able to provide a flattop shaped beam (e.g., [7]), to the best of the authors' knowledge there are no previous contributions as to obtain a flattop shaped beam in wide-band conditions. As far as the synthesis of the weighting window in wide-band conditions is concerned, the purposes of the previous papers [6,8-10] consisted of optimizing the side lobe profile, the side lobe peak, the side lobe energy, and the ratio between the main lobe energy and the side lobe energy. Besides the reduction of both the number of the elements composing the array and the spatial aperture has been dealt with [9,10]. However, none of the previous papers tackled with the optimization of the main lobe shape. Therefore, the proposed methods are not of any help to reach our goal.

To attain the optimization of the main lobe shape, an array synthesis process based on the simulated annealing (SA) has been developed. SA algorithm has been chosen because it represents a suitable approach to minimize the energy function that we defined and which is characterized by many local minima. The result of this procedure is a weighting window able to produce a BP that performs the applied constraint. Although the SA concept has already been used in this context (see the papers mentioned above dealing with the wide-band BP optimization), some essential changes are here introduced that are essential to successfully obtain the shaping of the main lobe. The related results are then described and discussed.

As the main lobe width shows a strong link to the angular resolution, the possibility to regulate the main lobe characteristics allows to establish the *a priori* performances of any acoustic imaging system. In particular, a BP with a flattop main lobe allows to produce a constant coverage over a given angular sector that is useful when a large area must be analyzed using a limited number of beams.

The paper is organized as follows. Section II contains the definition of the wide-band BP that we have used in our research; in Section III the energy function used for the synthesis of the weights and the details of the optimization procedure are described; Section IV deals with the discussion of the results; finally, in Section V some conclusions are drawn.

II. WIDE-BAND BP

Since the conventional definition of the BP is not valid any more in wide-band conditions, a redefinition is needed.

0-933957-31-9

Assuming that the acoustic waves received from a given incidence angle by each sensor of the array to be plane (far-field hypothesis), the received signals can be modeled as a replica of the transmitted pulse delayed on the base of the incidence angle and the positions of the linear array elements [4]. Let t indicate the time, θ the incidence angle of the plane wave, θ_0 the steering direction, and u the arbitrary variable (defined as $u = \sin\theta - \sin\theta_0$) that ranges in [-2, 2]. The angle of incidence and the steering angle are both measured according to the perpendicular to the array baseline. Once determined that the array is composed of M point-like omnidirectional elements, the beam signal, $b(t,u)$ can be computed as follows:

$$b(t,u) = \sum_{i=0}^{M-1} w_i \cdot A\left(t + \frac{idu}{c}\right) \cdot \exp\left(j\omega \frac{idu}{c}\right) \tag{1}$$

where w_i is the weight coefficient given to the i-th element, $A(t)$ is the envelope of the transmitted acoustic pulse (possibly after pulse compression), d is the inter-element spacing among the array sensors (pitch), ω is the angular frequency (computed as $\omega = 2\pi f_c$, where f_c is the carrier of the transmitted pulse), and c is the sound velocity in the medium considered. The exponential term in (1) reminds that a base-band quadrature reception has been hypothesized, thus the representation of the signals in terms of envelope and phase information is required [1]. In the near-field hypothesis, (1) is a valid approximation (through the Fresnel approximation) for the beam signal computed by a perfectly focused beamforming algorithm, provided that the focusing distance is equal to the real distance of the imaged reflecting point.

Of all the possible definitions, in our research the BP, $bp(u)$, has been computed, for a given pair of incidence and steering angles, as the maximum over the time of the beam signal:

$$bp(u) = \max_t \{|b(t,u)|\} \tag{2}$$

It can be observed that the function $bp(u)$ is equal to $bp(-u)$, hence it is sufficient to study and visualize the BP over the range $0 \le u \le 2$. Besides, it can be proved that when the wide-band hypothesis is relaxed until a narrow-band condition is achieved, the resulting BP is equal to the conventional narrow-band BP [4].

According to [4], the BP definition in (2) seems to be more suitable in the acoustical imaging, where the amplitude of the whole beam signal is reported along a line of pixels. The BP can also be defined as the square root of the total energy of the beam signal: this appears the right choice for applications where the total energy is used to perform further operations, e.g. detection [4]. To carry out our study, during the optimization process the BP has been normalized as follows:

$$bp_{norm}(u) = \frac{bp(u)}{\left|\sum_{i=0}^{M-1} w_i\right| \cdot A_m} \tag{3}$$

where A_m is the maximum over the time of the pulse envelope $A(t)$, $A_m > 0$. Finally, the conventional visualization of the BP on a logarithmic scale normalized to 0 dB is obtained as follows:

$$bpp(u) = 20\log[bp_{norm}(u)] \tag{4}$$

III. WEIGHT SYNTHESIS BY SA

The weight coefficients synthesis method proposed in this paper is based on the simulated annealing scheme. SA is a stochastic procedure to solve combinational minimization problems. The use of any optimization process requires the choice of an energy function to be minimized. SA is suitable when this function is nonlinear, has many variables, and, above all, has a large number of local minima. More details on the concept and implementation of SA can be found in [11].

The energy function $f(\mathbf{W})$ adopted in our paper depends on the weight vector $\mathbf{W}$ in order to be optimized. Once the desired normalized BP, $bp_d(u)$, has been determined, the energy function affects the array configurations that shows a considerable difference between the desired BP and the current one. Therefore, one can choose:

$$f(\mathbf{W}) = \left[k_1 \cdot \int_{u \in S_{ML}} |bp_{norm}(u) - bp_d(u)| du + (1-k_1) \cdot \int_{u \in S_{SL}} bp_{norm}(u) - bp_d(u) du\right]^2 \tag{5}$$

$$S_{ML} = \{u : 0 \le u \le u_{init}\}$$

$$S_{SL} = \{u : [bp_{norm}(u) > bp_d(u)] \cap [u_{init} < u \le u_{stop}]\}$$

Equation (5) shows that the energy function is composed of two terms: the first integral assesses the difference between the obtained BP and the desired one as to all the values of the u in the main lobe region, S_{ML}, while the second integral represents the areas of the side lobes region (S_{SL}) in which the obtained BP exceeds the desired one. If the energy function is lowered to zero, the constraints will be perfectly fullfilled. Along with allowing us to follow the main lobe BP used as constraint, the two integrals make us attain side lobes which are lower than the maximum level allowed. This is the reason why the first integral contains the absolute value of the difference between the actual and the desired BPs and is computed over the whole interval [0, u_{init}], while the second integral is just computed in the intervals in which the actual BP exceeds the desired one. In other words, one decides to carefully follow the main lobe of the desired BP, while it is sufficient that the side lobes of the actual BP stay under a given level, defined by the value of the desired BP in the interval [u_{init}, u_{stop}]. The parameter k_1, $0 \le k_1 \le 1$, allows to establish the relative importance of the two integrals that is the same when k_1 = 0.5. The parameter u_{init} defines where the main lobe region ends and the side lobe region begins, whereas u_{stop} defines where the side lobe region loses interest in relation to the application concerned.

One can make sure that the above energy function has many local minima; therefore, classical methods of local descent are not suitable for the minimization of this function, while SA because of its probabilistic nature is appropriate for being applied.

The flow chart below (Fig. 1) shows the optimization procedure. When the iteration j is started, the element i is randomly chosen (all the elements are visited according to a random sequence that does not allow any further visit of the same elements until they have been all visited once), its weight w_i is perturbed and, on the basis of the temperature T_j, the perturbation can be accepted or not. The chosen initial temperature, T_{start}, is high enough to allow the first configuration perturbations to be frequently accepted, even though they lead to a sharp energy increase.

During the optimization procedure no restrictions to limit the values of the weight coefficients are applied. The only limit is related to the quantity of the perturbation applied by the SA to each sensor over each iteration (i.e., ±0.1). In this way, the optimal weight configuration could reveal positive and negative coefficients that might be necessary in order to obtain the shape of the desired main lobe.

The number of iterations (j) increases every time all the M elements are perturbed once. The process stops when a state of persistent block (freezing) is reached due to the temperature decrease. Alternatively, according to the previous experience, one can perform a number of iterations large enough to ensure that a block state will be reached.

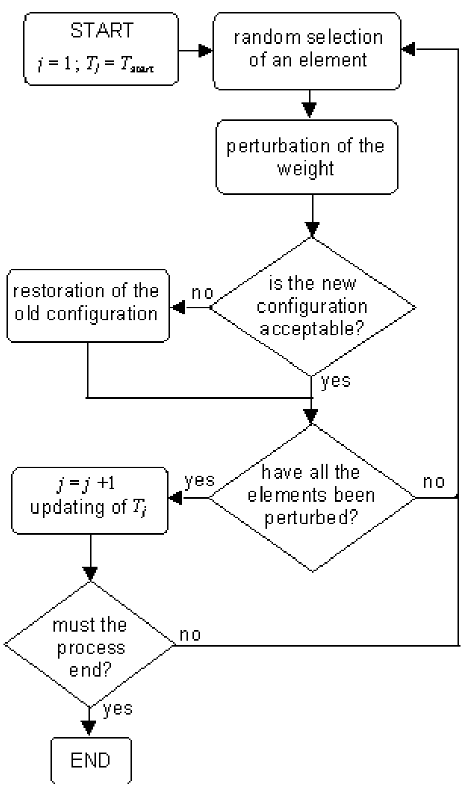

Fig. 1. Flow chart of the proposed optimization scheme.

Due to the probabilistic nature of SA, a different temperature scheduling and random initial configurations may lead to different final results. However, if a logarithmic scheduling is chosen, almost all the process runs give slightly different results in terms of energy and weight values. This means that the resulting weighting window is stable and close to the optimal one.

As compared to the algorithms for array synthesis in narrow-band conditions and based on SA - proposed by one of the authors in [12,13] - the computational load of the proposed method, in the wide-band hypothesis, is higher, due to the fact that the evaluation of the BP requires the computation of a whole beam signal for each u value. Besides, the BP must be computed (or simply updated) after each weight perturbation. Thus, one run of the proposed method may take a few hours computing time, but once the result is achieved, it is not necessary to run the algorithm any longer as the obtained weight values can be loaded into the imaging device, without requiring any re-computation.

IV. RESULTS AND COMPARISONS

To test the effectiveness of the proposed method, 2 different cases have been examined. In the first case, a linear λ/2-spaced array composed of 40 elements has been considered. The acoustic pulse was defined as a carrier frequency of 2.5 MHz whose amplitude was modulated by a truncated Gaussian envelope lasting 5.25 µs, with a variance equal to $3.5 \cdot 10^{-14}$ (i.e., a fractional bandwidth equal to 80%). The sampling frequency of the signals was fixed at 20 MHz during the optimization stage and at 200 MHz for result-testing and BP-visualization purposes. Regarding the SA scheme, the initial temperature was set as $T_{start} = 10.0$ and the number of iterations was equal to 2500.

In the conditions describes above, we tried to obtain the so-called "shaped beam", a typical BP in which the main lobe presents a flat top instead of a rapid descent. To this end, the desired BP used as constraint in the optimization process has been built by copying the shaped main lobe of a BP obtained in narrow-band conditions with the method proposed in [7]. Instead, the side lobe region has been determined equal to –25 dB. Figure 2 shows a comparison between the shaped BP obtained in [7] in narrow-band and the desired BP used in the optimization proposed in this paper. The reason why the side lobe level imposed in the desired BP is 5 dB higher than the side lobe level of the narrow-band shaped BP is due to the grating lobe in $u = 2$ that is found in narrow-band and will surely not be in wide-band [3,4]. Although the well-known equation of the total BP area is not applicable in wide-band conditions, the experience leads to the conclusion that the absence of such a grating lobe causes the side lobe to be higher than in the narrow-band case. Parameters have been defined as follows: $u_{init} = 0.3$, $u_{stop} = 1.2$, $k_1 = 0.75$.

The choice of limiting the optimization interval at $u_{stop} = 1.2$ is a consequence of the assumption that the sonar system

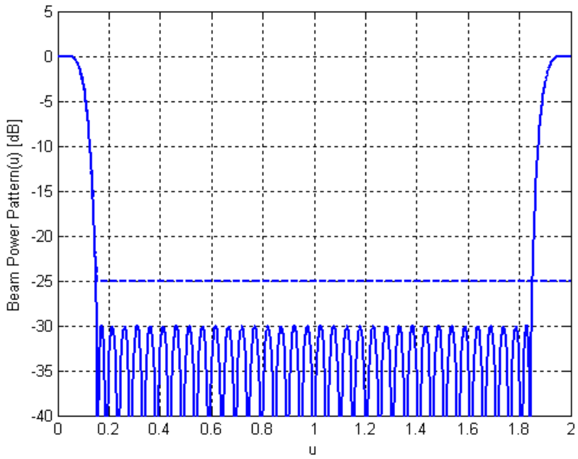

Fig. 2. Comparison between narrow-band shaped BP (solid line) and the desired BP (dash line).

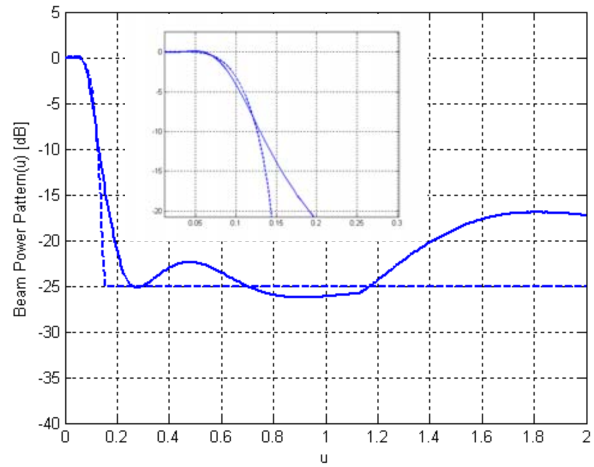

Fig. 3. Comparison between the wide-band BP obtained by the optimization process (solid line) and the desired BP (dash line). The inner chart shows magnified graph of the main lobe region.

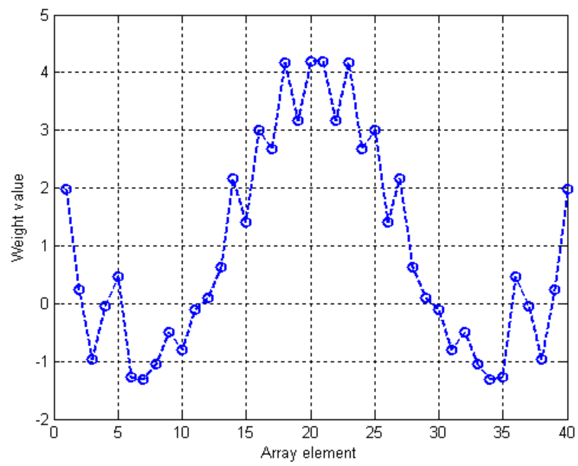

Fig. 4. Optimized weight coefficients. The circles refer to the λ/2-spaced element positions.

concerned has an insonification angle and a steering angle that range in [-37°, 37°]. For this reason, u values which are larger than 1.2 are not used in such a system. The restriction of the optimization interval at u_{stop} = 1.2 allows a free increase of the side lobes level in u > 1.2. This fact is appreciated for two reasons: (1) even though in u = 2 a true grating lobe will not be existing in the wide-band BP, a certain increase of the side lobe level is expected in the region close to u = 2, as predicted in [3,4]; (2) the increase of the side lobes in u > 1.2 might help to respect the constraints imposed in $u \le 1.2$.

Figure 3 shows one of the results obtained by the proposed method in comparison to the desired BP, $bp_d(u)$. The inner chart in Fig. 3 shows magnified graph of the main lobe region. Note that the main lobe obtained by the proposed method is close to the desired one and, above all, the 2 main lobes are essentially equal from 0 to –10 dB. In particular, the desired flat top is satisfactorily obtained in the wide-band BP. The side lobe region is not completely contained under the –25 dB constraint; however, differences are fairly limited, being they bounded to a couple of dB. Finally, as expected, when $u \ge 1.2$ the side lobes level grows freely.

Figure 4 shows the values of the optimized weight coefficients and the (interpolated) profile of the resulting window. Similar profiles are obtained by performing many runs of the optimization method, with the same desired BP.

Examining Fig. 4, one can observe that the weighting window is symmetric compared to the central element of the array. During the first runs of the optimization process, we have observed that the optimal windows obtained by the SA showed a slightly symmetric profile. Therefore, a symmetric profile has been imposed *a priori*, reducing the computational load of the optimization process by 30%. Besides, like in the narrow-band case [7], some coefficients of the window are negative.

In the second test case a linear λ/2-spaced array composed of 50 elements has been considered. The acoustic pulse and the sampling frequency were the same as the ones used in the first case along with the SA parameters. In this second case we tried to obtain the same main lobe characterizing the narrow-band BP provided by a Dolph-Chebyshev window. In particular, the main lobe of the desired BP is the same as the narrow-band BP obtained by the Dolph-Chebyshev window equalized at –35 dB. Instead, the side lobe region has been determined as equal to –32 dB. Figure 5 shows a comparison between the narrow-band BP obtained by the window mentioned above and the desired BP. The reason why the side lobe level imposed in the desired BP is higher than the equalizing level of Dolph-Chebyshev window is, as in the first case, related to the grating lobe in u = 2. The parameters have been determined as follows: u_{init} = 0.1, u_{stop} = 1.4, k_1 = 0.90. The choice of limiting the optimization interval at u_{stop} = 1.4 is a consequence of the assumption that the sonar system concerned has an insonification angle and a steering angle that range in [-45°, 45°].

The comparison between the imposed constraint and the BP obtained by the weighting window optimized by the

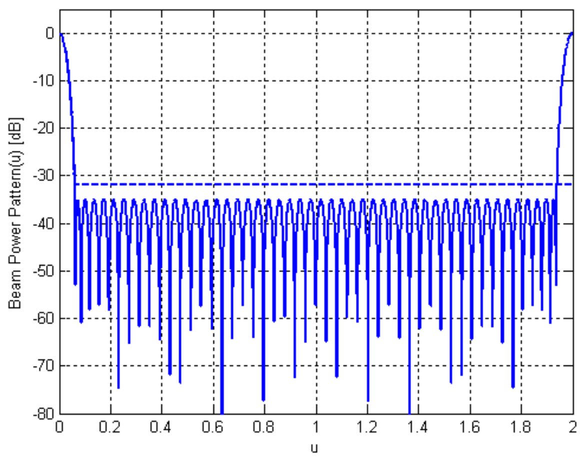

Fig. 5. Comparison between the narrow-band BP obtained by the Dolph-Chebyshev window equalized at –35 dB (solid line) and the desired wide-band BP (dash line).

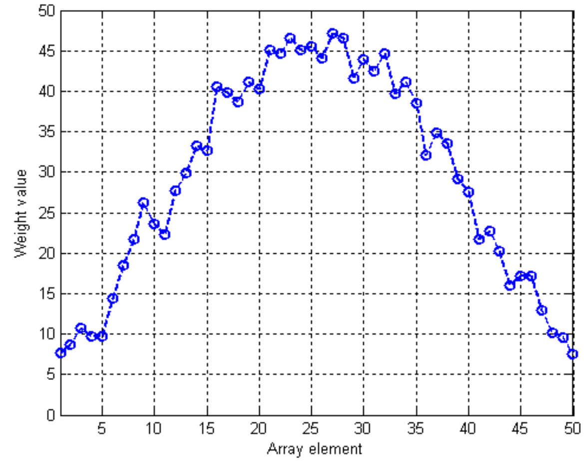

Fig. 7. Optimized weight coefficients. The circles refer to the λ/2-spaced element positions.

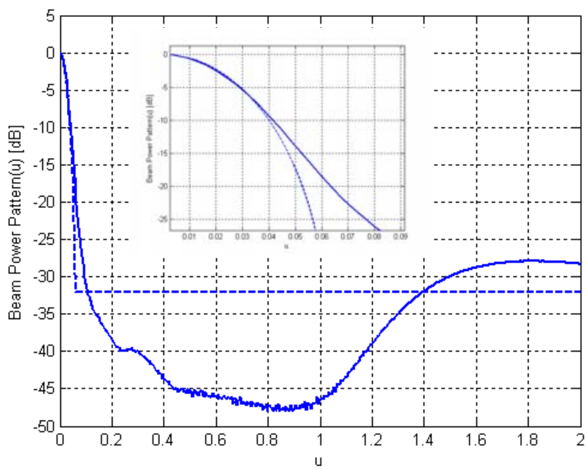

Fig. 6. Comparison between the wide-band BP obtained by the optimization process (solid line) and the desired BP (dash line). The inner chart shows magnified graph of the main lobe region.

	Flat top ML		Dolph-Chebyshev ML	
	Width [u]		Width [u]	
dB level	Optimized	Desired	Optimized	Desired
-3	0.094	0.099	0.022	0.023
-6	0.111	0.114	0.032	0.032
-10	0.130	0.126	0.042	0.040
-15	0.157	0.137	0.053	0.047
-20	0.191	0.144	0.063	0.052

Table 1. Comparison between the desired and the obtained BPs in terms of main lobe (ML) width, evaluated at different levels, for the 2 shown cases.

proposed method is shown in Fig. 6. The inner chart represents the magnified graph of the main lobe region. Note that in this case too the main lobe obtained by the proposed method is close to the desired one and, in particular, the 2 main lobes are equal when their value ranges from 0 to –10 dB. For lower levels, the obtained main lobe is slightly larger than the desired one. The side lobe region is completely contained under the –32 dB constraint. Finally, when $u \geq 1.4$ the side lobes level grows freely as expected.

The values of the weight coefficients provided by the proposed method are shown in Fig. 7. In this case, despite the symmetry constraint was not set, a quasi-symmetric window was obtained as a natural result of the optimization procedure.

Observing Fig. 3 and 6, it is clear how much the proposed technique allows generating BPs with a main lobe shape which is very close to the desired one. Not only is a desired generic shape achieved, but also the main lobe width values, measured at different levels, are very close to the desired ones. In particular, as summarized in Table 1, the width values are essentially the same when their range from –3 to –10 dB, and similar when their value is below –10 dB, where the obtained main lobes are always slightly larger than the imposed ones.

The main problem associated with the proposed method is that it is difficult to in obtain a total overlapping between the optimized BP and the desired one for the whole main lobe region. In fact, in both cases, below –10 dB there is a triangular area that represents the difference between the desired main lobe and the main lobe generated by the weighting window synthesized by our approach. Even if many efforts to decrease the triangular difference have been made (increasing k_1, and the desired side lobe level, decreasing the value of u_{stop}), the results shown in this paper represent the best outcome obtained. Our current opinion about the difficulty in reducing the triangular difference is that it might be due to a theoretical (unknown) limit related to the wide-band nature of the addressed BPs which is still to be investigated.

V. CONCLUSIONS

In this paper, it has been proposed a method aiming at synthesizing the values of the weight coefficients to be applied to the elements of a linear array working in wide-band conditions that generate a BP with the main lobe equal to a desired one and the side lobes kept at a maximum level allowed. Such a method relies on a stochastic scheme that has been based on the SA algorithm. The main implementation details have also been discussed.

In particular, we tried to reproduce a couple of special cases taken from the narrow-band practice in wide-band conditions: the main lobe of a flattop shaped BP and the main lobe produced by a Dolph-Chebyshev window. Although the quality of the obtained BPs, in terms of main lobe profile and side lobe peak, has been slightly poorer than that of the narrow-band templates, the proposed method allowed to obtain satisfactorily the desired main lobe shape in both tests. Because of these results, we can conclude that the devised technique represents a very useful innovative tool to generate a wide-band BP with a desired main lobe profile.

REFERENCES

[1] R.O. Nielsen, *Sonar Signal Processing*, Artech House, Boston, 1991.

[2] V. Murino, A. Trucco, "Three-Dimensional Image Generation and Processing in Underwater Acoustic Vision, " *The Proceedings of the IEEE*, vol. 88, pp. 1903-1946, December 2000.

[3] A. Macovski, "Ultrasonic Imaging Using Arrays," *IEEE Proceedings*, vol. 67, pp. 484-495, April 1979.

[4] V. Murino, A. Trucco, and A. Tesei, "Beam Pattern Formulation and Analysis for Wide-Band Beamforming Systems Using Sparse Arrays," *Signal Processing*, vol. 56, no. 2, pp. 177-183, January 1997.

[5] J.L. Schwartz and B.D. Steinberg, "Ultrasparse, Ultrawideband Arrays," *IEEE Trans. Ultrasonics, Ferroelectrics, and Frequency Control*, vol. 45, no. 2, pp. 376-393, March 1998.

[6] G. Cardone, G. Cincotti, and M. Pappalardo, "Design of Wide-Band Arrays for Low Side-Lobe Level Beam Patterns by Simulated Annealing," *IEEE Trans. on Ultrasonics, Ferroelectrics, and Frequency Control*, vol. 49, no.8, pp. 1050-1059, August 2002.

[7] L. Wu, A. Zielinski, J.S. Bird, and R. Kieser, "Synthesis of Symmetric Flattop Radiation Patterns," *IEEE Journal of Oceanic Engineering*, vol. 21, no. 1, pp. 105-108, January 1996.

[8] A. Trucco, "A Stochastic Approach to Optimise Wide-Band Beam Patterns," in *Acoustical Imaging, Volume 25*, M. Halliwell and P.N.T. Wells, Eds. New York: Kluwer Academic/Plenum Press, 2000, pp. 123-130.

[9] G. Cardone, G. Cincotti, P. Gori, and M. Pappalardo, "Optimization of Wide-Band Linear Arrays," *IEEE Trans. on Ultrasonics, Ferroelectrics, and Frequency Control*, vol. 48, no. 4, pp. 943-952, July 2001.

[10] A. Trucco, "Weighting and Thinning Wide-Band Arrays by Simulated Annealing," *Ultrasonics*, vol. 40, nos. 1-8, pp. 485-489, March 2002.

[11] S. Kirkpatrick, C.D. Gellatt Jr., and M.P. Vecchi, "Optimization by Simulated Annealing," *Science*, vol. 220, no. 4598, pp. 671-680, 1983.

[12] A. Trucco, V. Murino, “Stochastic Optimization of Linear Sparse Arrays,” *IEEE Journal of Oceanic Engineering*, vol. 24, pp. 291-299, July 1999.

[13] V. Murino, A. Trucco, and C.S. Regazzoni, "Synthesis of Unequally Spaced Arrays by Simulated Annealing", *IEEE Trans. Signal Processing*, vol. 44, no. 1, pp. 119-123, January 1996.